PHILOSOPHICAL TRANSACTIONS OF THE ROYAL SOCIETY A MATHEMATICAL, PHYSICAL & ENGINEERING SCIENCES

The creation and study of Bose-Einstein condensation in a dilute atomic vapour

C. E. Wieman

Phil. Trans. R. Soc. Lond. A 1997 **355**, 2247-2257
doi: 10.1098/rsta.1997.0123

The creation and study of Bose–Einstein condensation in a dilute atomic vapour

By C. E. Wieman

JILA and Department of Physics, University of Colorado, Boulder, CO 80309, USA

I will discuss the work of the JILA/University of Colorado group on the creation and study of Bose–Einstein condensation (BEC) in a gas of very cold rubidium atoms. Over the years, a large number of students and postdocs have contributed to this work, with Eric Cornell and myself as the coleaders of the project. The data reported in this paper were obtained by Mike Anderson, Eric Burt, Jason Ensher, Rich Ghrist, Deborah Jin, Mike Matthews and Chris Myatt. Theoretical contributions have been provided by Murray Holland, Jinx Cooper, Brett Esry and Chris Greene. In the first part of this paper, I will briefly discuss how we create and observe BEC; in the second portion, I will discuss some of the work on BEC that has been carried out at JILA in the past year.

1. Bose–Einstein condensation in a gas (1924–1995)

Although all the constituents of atoms (neutrons, protons and electrons) are fermions, if they are assembled such that the total spin of the atom is an integer and the atoms remain far apart compared to the size of their electron clouds, they will behave as weakly interacting bosons. The first discussion of the energy distribution of such bosonic atoms when placed in a container was given by Einstein in 1924 (Einstein 1924, 1925). For a macroscopic container, the spacing between quantized energy levels is extremely small and thus at normal temperatures the atoms are distributed over a large number of different levels. At finite but very low temperatures, however, the Bose–Einstein distribution formula predicts a large fraction of the atoms will go into the lowest energy level of the container (figure 1). This is known as Bose–Einstein condensation. The condition for this to happen is that the atomic phase space density must be so large that the de Broglie wavelengths of the cold atoms are greater than the interparticle spacing.

The primary motivation for our work was to explore this macroscopic quantum behaviour of BEC in a gas, and to compare and contrast it with that of the other macroscopic quantum states we know, particularly superfluid helium. (In addition to superfluid helium, two other examples are superconductivity and BEC in excitons. The latter is discussed in Lin & Wolf (1993). For a discussion of BEC in many different systems, see Griffin *et al.* (1995).) Being a liquid, helium is quite different from the ideal gas discussed by Einstein. Because the atoms are very close together in the liquid, this is a strongly interacting system. These strong interactions are actually responsible for much of the interesting behaviour we associate with superfluid helium, but the interactions also make it much more difficult to understand the macroscopic

Phil. Trans. R. Soc. Lond. A (1997) **355**, 2247–2257
Printed in Great Britain

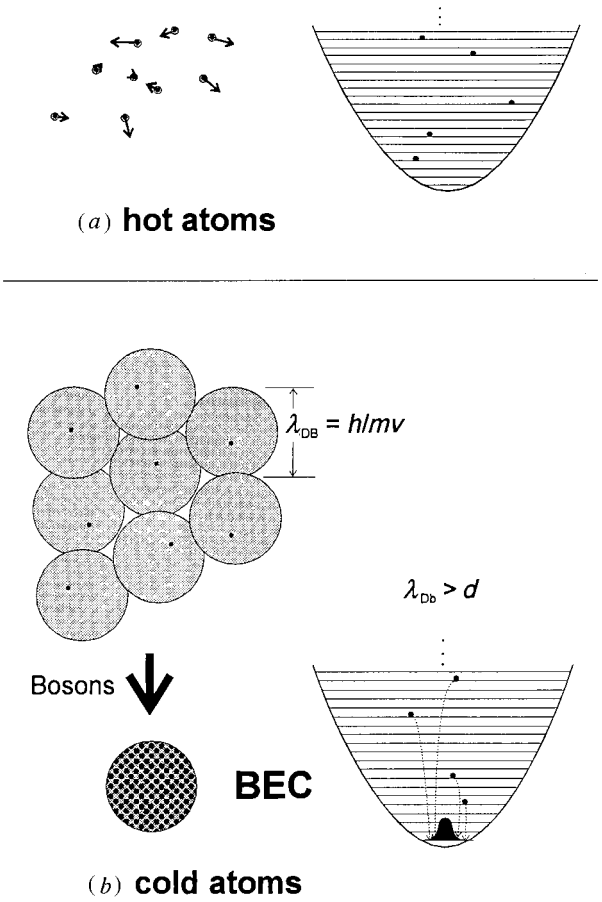

Figure 1. (*a*) Distribution of hot atoms over the quantized energy levels in a macroscopic container. (*b*) When bosons are cooled sufficiently that the de Broglie wavelength, λ_{Db}, is larger than the spacing between atoms, d, the atoms fall into the lowest energy state in the potential.

properties of superfluid helium in terms of the microscopic interaction between two helium atoms.

BEC in an alkali vapour is nearly the perfect tool for exploring how the microscopic interactions between atoms lead to the macroscopic properties of the many-atom quantum state. Because the atoms in the condensate are far apart compared to their atomic size, the interactions are weak and well understood. Furthermore, we can readily adjust these interactions in experiments by a variety of means, the simplest of which is simply to change the density of the gas. Finally, we have very good optical diagnostics for looking at the condensate and measuring its properties. This combination of factors make this an excellent system for studying in detail how one goes from the microscopic to the macroscopic in such a quantum system. A gaseous BEC is also interesting in that it is the atomic analogue to laser light and shares the primary feature that makes laser light useful, namely very high phase space number density.

The principal difficulty in producing BEC in a gas is that, at the necessary low densities, the BEC transition temperature will be very low, on the order of 100 nK.

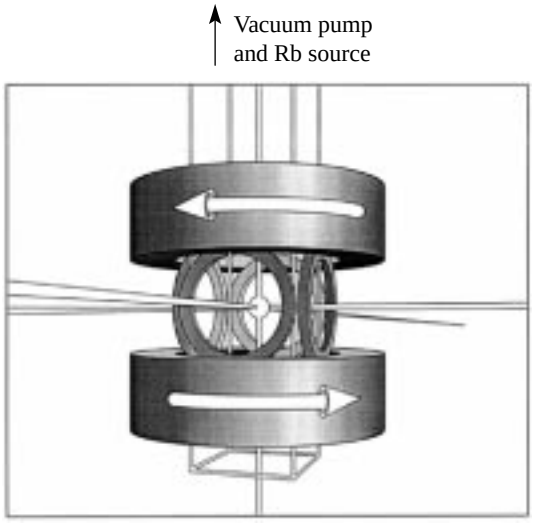

Figure 2. BEC trapping cell. A rectangular glass cell (2.5 cm square by about 10 cm high) is attached to a vacuum pump and rubidium reservoir (not shown). Laser beams coming from all six directions go through the cell. The magnetic fields are produced by the two large coils and the four smaller coils.

Obviously this is a major technical challenge, but there is also the fundamental difficulty that at this temperature all atoms want to be a solid rather than a gas. The solution to this problem is to 'cheat' thermodynamics by creating a system with two very different time scales. The first is the time for the gas to come to thermal equilibration as a gas, and this should be very short. The second time scale is the time required for the vapour to go to its true equilibrium ground state (a solid), and this must be very long. Thus the gas will remain in its metastable super-saturated-vapour state for a long time, during which it can Bose condense.

These considerations led us to the idea that these conditions could be satisfied by cooling alkali atoms by the combination of two different technologies: laser cooling and trapping (Wieman & Chu 1989; Arimondo *et al.* 1992; Newbury & Wieman 1996) and magnetic trapping and evaporative cooling. (For a review of the hydrogen work, see Greytak (1995) and references therein.) These two technologies had been developed by the efforts of many groups over the past 20 years. The former were motivated by the desire to find new ways to manipulate atoms using laser light, while the latter arose from the efforts to obtain BEC in a gas of spin polarized hydrogen. Our own work on BEC grew out of our studies in the late 1980s of the processes that limited the temperatures and densities one could achieve in laser trapped and cooled samples. We discovered several processes arising from the multiple scattering of photons were responsible (Sesko *et al.* 1989, 1991; Walker *et al.* 1990). To overcome these limits, we turned off the laser light and then put our laser cooled and trapped atoms into a magnetic trap. Inspired by the hydrogen work, we then evaporatively cooled these samples.

The heart of the apparatus we used to first produce BEC is shown in figure 2 (Anderson *et al.* 1995). A magneto-optic trap (MOT) is created inside a glass vapour cell in the usual manner using light from diode lasers (Monroe *et al.* 1990). This provides an enormous increase in the phase space density (10^{16}), but leaves us about 10^5 away from BEC. These atoms are then loaded into the magnetic trap. The magnetic trap uses the interaction between the magnetic moments of the atoms

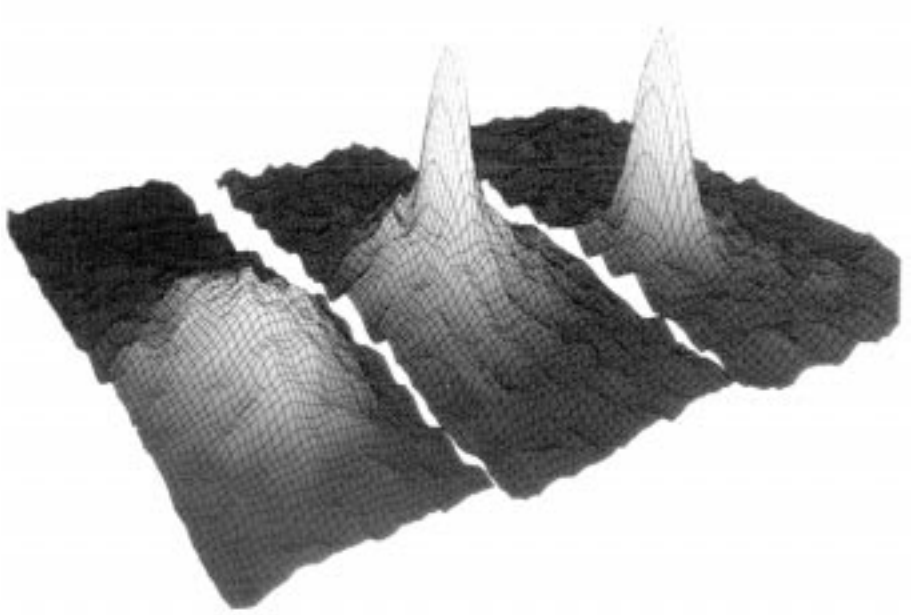

Figure 3. Two-dimensional velocity distributions of the trapped cloud for three experimental runs, corresponding to temperatures of (left to right) 200, 100 and *ca.* 0 nK. The axes are the x and z velocities, and the number density of atoms per unit velocity-space-volume. This density is extracted from the measured optical thickness of the shadow. The original colour versions can be seen on the JILA WWW home page at `http://jilav1.colorado.edu/www/bose-ein.html` and on the 1996 APS calendar.

and an appropriately configured inhomogeneous magnetic field to confine the atoms. In evaporative cooling, the most energetic atoms are allowed to escape out of the potential well, and in doing so they carry off more than their share of the energy. This leaves the remaining atoms colder. This is exactly how a cup of coffee cools—the energetic coffee molecules leap out of the cup into the room. In the hydrogen experiments that first demonstrated evaporative cooling, as in our experiments, the edge of the potential well over which the atoms escape is slowly lowered as the sample is cooled, thereby continually cooling the sample to lower and lower temperatures. The final temperature in the evaporative cooling is set by the final level of the potential.

To observe the cooled sample, we turn off the magnetic fields, allowing the atoms to fly apart. We then take a 'shadow snapshot' of the expanded cloud. This image is obtained by illuminating the expanded cloud with a very short pulse of laser light which is tuned to the resonant frequency of the atoms. The atoms absorb the light, thereby casting a shadow in the illuminating laser beam, and this shadow is imaged onto a CCD array (TV camera). This shadow image is the two-dimensional projection of the velocity distribution of the original cloud of atoms in the magnetic trap. From the velocity distribution we can extract the temperature and various other properties of the sample.

A set of three such pictures is shown in figure 3 (Anderson *et al.* 1995). These pictures correspond to three repetitions of the experiment, where the only difference is the amount of evaporative cooling. In the picture on the left, we have only cooled the atoms down to 400 nK, and what we see is a round hill, which looks like the familiar Maxwell–Boltzmann velocity distribution. At higher temperatures (not shown here),

the cloud has the same shape with a larger width. The middle picture shows a cloud (*ca.* 10 000 atoms) where the sample was cooled further, down to about 200 nK. On top of the rounded hill, a narrow spire has emerged which is centred at zero velocity. If we cool even further (right picture), we can produce a sample (*ca.* 2000 atoms) in which the hill is completely gone and only the narrow spire remains visible.

You can see how this behaviour is exactly what one expects for BEC if you go back to the original concept. The normal atoms that are distributed over many energy levels form the Maxwell–Boltzmann-like hill. The atoms in the lowest energy state of the harmonic trapping potential are the most localized in both position and velocity space, and they are centred at zero velocity. Thus as atoms condense into that state they form a very narrow peak in the velocity distribution, which sits on top of the broader hill of non-condensed atoms.

Other features of these velocity distributions also indicate that we are seeing BEC. One is the peak density of the trapped cloud as a function of temperature. This density is nearly constant as the temperature is lowered, until the transition temperature is reached. The density then changes dramatically, increasing by a factor of 100 within 75 nK. This provides a strong indication of a phase transition. Another interesting aspect of the condensate is revealed by looking down on the peaks of figure 3 from above, as shown in figure 4. Figure 4*a* shows that the contour lines of the rounded hill are circular, indicating an isotropic distribution for the thermal sample as required by the equipartition theorem; figures 4*b*, *c* show that the spires are not round but instead are quite elliptical, indicating an anisotropic velocity distribution. This elliptical distribution is an actual image of a macroscopic quantum wave function. It is elliptical because the shape of the wave function reflects the anisotropic shape of our harmonic trapping potential. These are the measurements we completed in June 1995 to establish that we had seen BEC in trapped rubidium. Since then we have carried out further measurements on the shape of this wave function, and how it changes as the interactions between the atoms is varied (by adjusting the density). These shapes agree very well with the theoretical predictions of Murray Holland (Holland *et al.* 1997).

Using different technology, but the same basic approach, Ketterle and coworkers at MIT clearly observed BEC in sodium in late 1995 (Davis *et al.* 1995), with substantially larger samples than we obtained in our first experiments. Recently, Hulet and coworkers have demonstrated BEC in lithium as well (Bradley *et al.* 1997).

2. BEC results (1996)

The remainder of this paper will discuss some of the recent measurements the JILA group has made on properties of the condensates and a second-generation apparatus that is now operating. The MIT group has also measured a number of related properties of condensates (Mewes *et al.* 1996*a*,*b*).

We have used the original BEC apparatus to carry out a series of measurements over the past year. These include studies of the collective excitations (Jin *et al.* 1996, 1997) of the condensate, measurement of the fraction of atoms in the condensate as a function of temperature (Ensher *et al.* 1996) and a determination of the specific heat of the sample as a function of temperature (Ensher *et al.* 1996). Here I will only discuss the collective excitations. To observe the phonon-like collective excitations, we use a technique that is very similar to the free induction decay method of NMR. We first apply a periodic perturbation to the condensate and then watch the con-

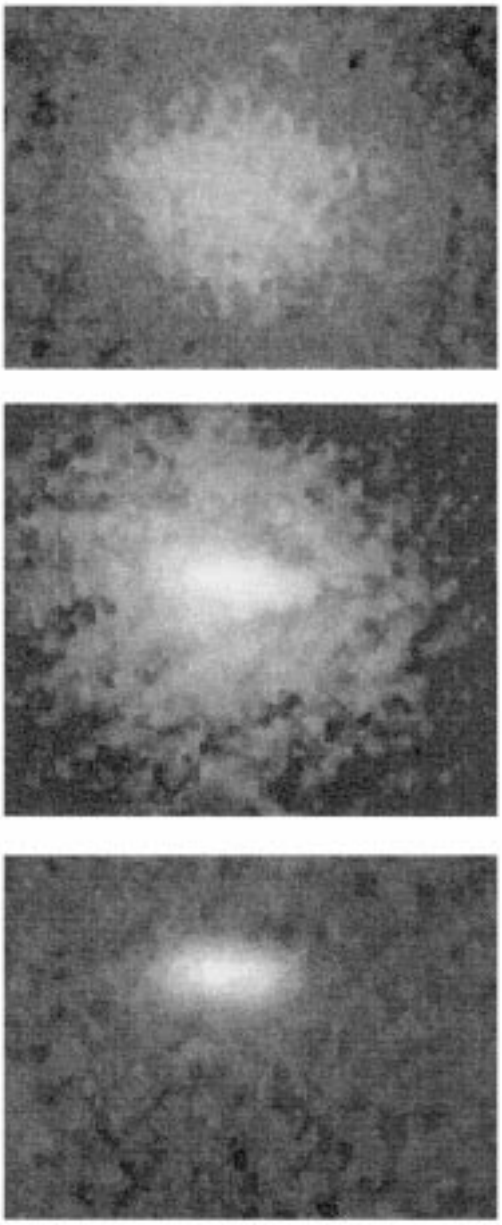

Figure 4. Two-dimensional plot of x and z velocity distributions of the samples shown in figure 3 (from Anderson *et al.* 1995). Images shown are negatives of actual data, so brighter corresponds to more atoms (less transmitted light).

densate oscillate freely after the perturbation is removed. The periodic perturbation is produced by applying time-dependent magnetic fields which gently squeeze the condensate. We have excited modes with two different symmetries. The monopole, or $m = 0$ mode, is excited by uniformly squeezing and stretching the condensate in the isotropic x–y plane. The quadrupole, or $m = 2$ mode, is excited by applying sinusoidal squeezes along the x and y directions which are 90° out of phase. This excites

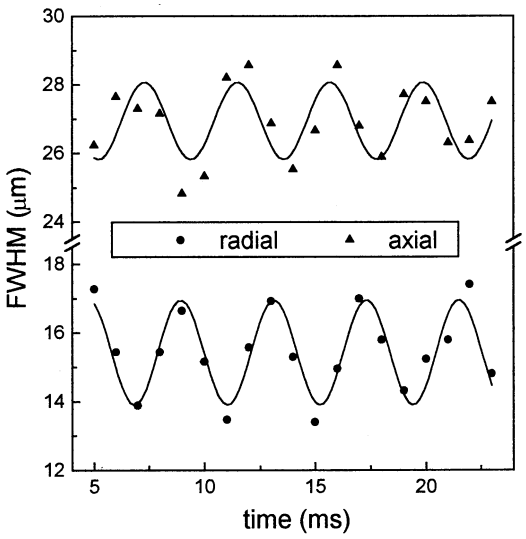

Figure 5. Time dependence of the radial and axial width of the condensate during the free oscillation period, after the $m = 0$ mode has been excited.

a mode corresponding to an elliptical distortion of the condensate that rotates in the plane. We wait varying lengths of time after the end of the perturbation before we release the cloud and look at it. This gives us the time dependence of the spatial distortion of the condensate. Figure 5 shows this distortion as a function of time. It can be seen that it is a very clean damped sinusoidal oscillation. By fitting this curve to a damped sine wave we determine the oscillation frequency and the damping time of the excitation.

We have measured the oscillation frequencies of the $m = 0$ and $m = 2$ modes as a function of the interactions in the condensate. The excitation frequencies are dramatically shifted from the value corresponding to a non-interacting gas, which is also the excitation frequency of the non-condensed trapped atoms. The observed condensate excitation frequencies at our lowest achievable temperatures (50 nK) agree well with theory over the full range of interaction strengths (Jin *et al.* 1996, 1997; also see Burnett paper in this volume). We have studied the frequencies and damping of these two modes as a function of temperature, and observe dramatic and surprising results. These are shown in figure 6. First, the frequencies of the two modes have very different temperature dependencies. The $m = 0$ mode is fairly flat, then has a small very narrow dip, and then as the temperature increases further, it rapidly rises up to the oscillation frequency of the uncondensed atoms in the trap. The $m = 2$ mode, in contrast, decreases monotonically as the temperature is increased. Perhaps the strangest aspect of these shifts is that they are comparable in size to the shifts observed in the low temperature condensates as we varied the density by a factor of 1.5. Here, however, we are adding a thermal gas component whose density is only a small fraction of that of the condensate and observing similar shifts. The two modes show essentially identical damping and it depends strongly on temperature. A surprising feature is that for temperatures slightly below the transition, the condensate oscillations damp much faster than comparable excitations in the normal gas. There are currently no explanations for either the temperature-dependent damping, or the frequency shifts we observe, but it is a subject of considerable current theoretical

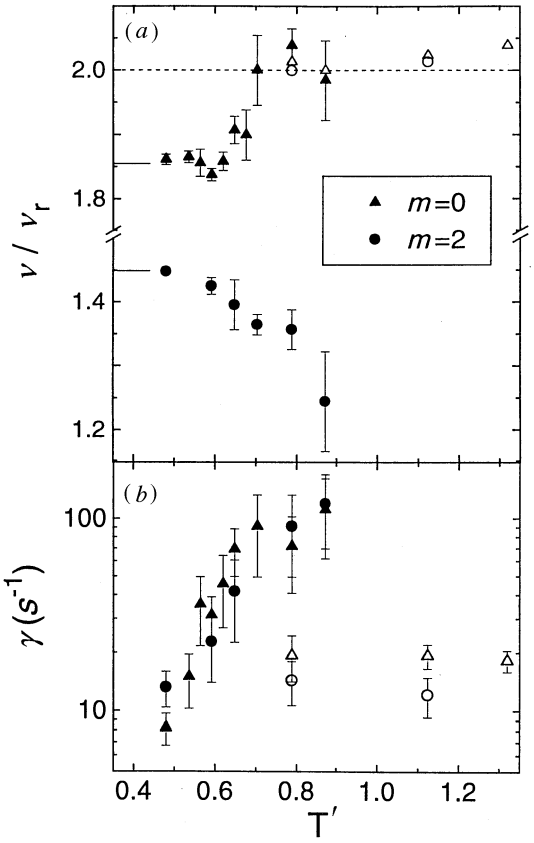

Figure 6. Temperature-dependent excitation spectrum. (a) Frequencies (normalized by the radial trap frequency) for $m = 0$ (triangles) and $m = 2$ (circles) collective excitation symmetries are shown as a function of normalized temperature T'. Oscillations of both the condensate (solid symbols) and non-condensate (open symbols) clouds are observed. Short lines extending from the left side of the plot mark and mean-field theoretical predictions in the $T = 0$ limit (for 6000 atoms in our trap). (b) For both the $m = 0$ and $m = 2$ condensate excitations, the damping rate γ quickly decreases with decreasing temperature. For each point in (b) there is a corresponding frequency in (a) determined from the same set of data.

activity. In the future, it will be interesting to study collective excitations of condensates further to examine the behaviour of higher frequency modes and the excitation of vortices. Ultimately, it should be possible to completely understand the quantum fluid dynamics of this system.

We have constructed a new apparatus (Myatt *et al.* 1997) which has some advantages over the original system. This apparatus uses the same basic principle but has two separate MOTs (Myatt *et al.* 1996). The first one is in an upper chamber that has a relatively high pressure of rubidium vapour. The second is in a differentially pumped lower chamber that has very low pressure. The two chambers are connected by a long narrow tube, and after the atoms are trapped in the upper chamber they are then given a small push which sends them down the tube to be caught in the lower MOT. The atoms will stay in the lower MOT for many hundreds of seconds and so we can load many such bunches of atoms into it. This allows us to start with many more atoms and have a longer trap lifetime for evaporative cooling. We then magnetically trap these atoms and evaporatively cool them. For the sake of variety,

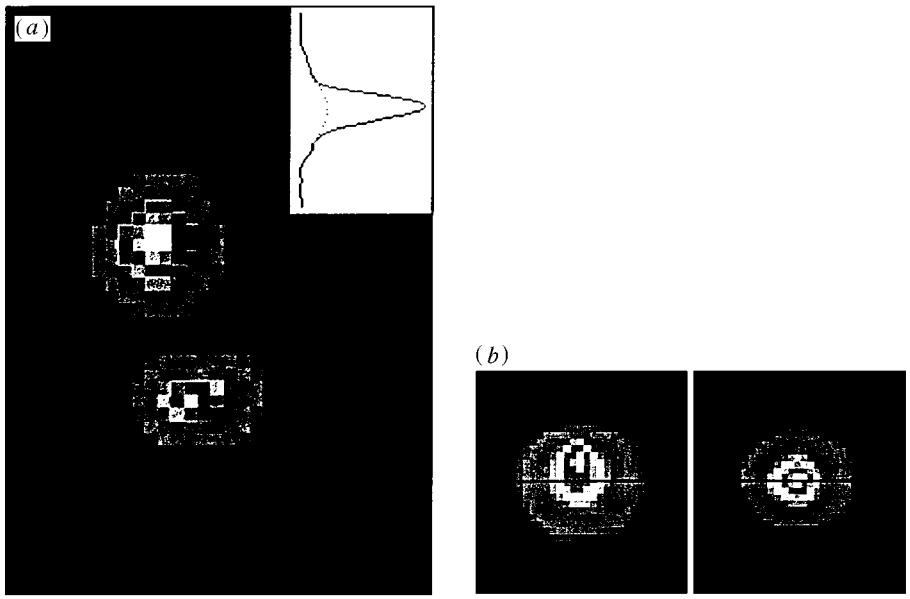

Figure 7. (*a*) An absorption image (475 μm by 675 μm) showing condensates of both $|2,2\rangle$ (left) and $|1,-1\rangle$ (right) states that were created simultaneously by sympathetic cooling. The condensates are separated because the trap axis was tilted 40 mrad to produce a component of the gravitational force along the weak spring constant direction. The non-condensed parts of the clouds (purple and dark blue) still overlap. The shape of both of the condensates is a function of expansion time, but the difference in their ellipticities reflects the fact that they have different initial confinements and therefore expand at different rates. The inset shows a vertical trace through the cloud on the left. The dotted line is to guide the eye in distinguishing the broad thermal background from the narrow condensate peak. (*b*) Two 475 μm by 475 μm false-colour absorption images of $|2,2\rangle$ atoms. Left: a cloud of two overlapping condensates illuminated so that only the $|2,2\rangle$ state atoms are visible. The condensate (white, red and yellow) is shifted upwards relative to the centre of the thermal uncondensed cloud (green, blue and purple) due to interactions with the $|1,-1\rangle$ condensate. The $|1,-1\rangle$ atoms are not visible in this image. Right: a cloud of pure $|2,2\rangle$ atoms cooled to a comparable temperature as in (*a*). The black line is a guide to the eye going through the centre of both thermal clouds.

we have used our old 'baseball coil' magnetic trap in this apparatus rather than the TOP trap used in our first BEC machine. This is not a fundamental difference in that the two types of traps appear to be fairly similar in their ability to produce condensates. They each have technical advantages and disadvantages for any particular experiment. In the new BEC apparatus we have now produced condensates containing about 2×10^6 atoms. Probably the most important aspect of this apparatus, relative to our first BEC apparatus, is that it still has the advantages of using simple and low cost diode laser and vapour cell MOT technology, but it provides a much greater ($\times 50$) safety margin for having sufficient collision rate to evaporatively cool to produce condensates.

As well as making experiments much easier, this has also allowed us to easily produce condensates in either or both of the $F = 2$, $m = 2$ and $F = 1$, $m = -1$ spin states of ^{87}Rb (Myatt *et al.* 1997). Somewhat surprisingly, when we examine condensates composed of either of the individual spin states, we see that they have very different heating and loss rates (nearly a factor of ten), with the $F = 2$ state atoms both heating more quickly and being lost from the trap faster. We have also

been able to create condensates composed of a mixture of these two spin states. This is shown in figure 7. We observe that there is a strong interaction between the two condensates that causes them to separate into two well-defined independent blobs. The $F = 1$ condensate pushes the $F = 2$ condensate out of its normal equilibrium position in the centre of the trap. All these features are rather striking if one considers that we are putting two dilute gases into a container, and, instead of mixing, they remain quite separate and exert substantial forces on these independent macroscopic bodies. This illustrates how the condensates are dramatically different from independent atoms.

We are currently studying collisional processes in these condensates. We observe that the dominant loss process is proportional to the cube of the density, indicating that it is three-body recombination of the rubidium atoms. A particularly interesting feature of this process is that, by comparing collision rates between condensed and uncondensed samples, it allows us to study the spatial correlations or fluctuations in the wave function. The observed rate constant is about six times larger in an uncondensed sample than it is in the condensate. This agrees with the factor of 3! that is predicted. This factor arises from the fact that the thermal sample has fluctuations, while the BEC is a coherent sample with no spatial fluctuations. Thus, for the condensate, the average of the density cubed is the same as the cube of the average density. For a thermal sample, however, it is six times larger.

Thus this confirms the coherent nature of the BEC wave function. The group of Ketterle (Andrews *et al.* 1997) has recently demonstrated this in a complementary manner. They have created two independent condensates and observed spatial fringes when the two are overlapped. This also demonstrates the long range coherence of the condensate samples. Nearly every experiment that has been carried out on BEC samples has offered new surprises or new questions to be explored. Our second generation apparatus allows one to create and study condensates on a relatively routine basis. It is clear that the study of Bose–Einstein condensates will be a rich field for many years to come.

This work has been supported by NSF, ONR and NIST.

References

Anderson, M. H., Ensher, J. R., Matthews, M. R., Wieman, C. E. & Cornell, E. A. 1995 *Science* **269**, 198–201.

Andrews, M. R., *et al.* 1997 *Science* **275**, 637–641.

Arimondo, E., Phillips, W. & Strumia, F. (eds) 1992 *Proc. Int. School of Physics 'Enrico Fermi'. Course CSVIII. Laser manipulation of atoms and ions.* Amsterdam: North-Holland.

Bradley, C. C., Sackett, C. A. & Hulet, R. G. 1997 *Phys. Rev. Lett.* **78**, 985.

Davis, K. B. *et al.* 1995 *Phys. Rev. Lett.* **75**, 3969–3973.

Einstein, A. 1924 *Sitzber. Kg. Preuss. Akal. Wiss.*, 261.

Einstein, A. 1925 *Sitzber. Kg. Preuss. Akad. Wiss.*, 3.

Ensher, J. R., Jin, D. S., Matthews, M. R., Wieman, C. E. & Cornell, E. A. 1996 *Phys. Rev. Lett.* **77**, 4984–4987.

Greytak, T. 1995 In *Bose–Einstein condensation* (ed. A. Griffin, D. Snoke & S. Stringari), p. 131. Cambridge University Press.

Griffin, A., Snoke, D. & Stringari, S. 1995 *Bose–Einstein condensation.* Cambridge University Press.

Holland, M. & Cooper, J. 1996 *Phys. Rev.* A **53**, R1954–1957.

Holland, M. J., Jin, D. S., Chiofalo, M. L. & Cooper, J. 1997 *Phys. Rev. Lett.* **78**, 3801.

Jin, D. S., Ensher, J. R., Matthews, M. R., Wieman, C. E. & Cornell, E. A. 1996 *Phys. Rev. Lett.* **77**, 420–423.

Jin, D. S., Matthews, M. R., Ensher, J. R., Wieman, C. E. & Cornell, E. A. 1997 *Phys. Rev. Lett.* **78**, 764–771.

Lin, J.-L. & Wolfe, J. P. 1993 *Phys. Rev. Lett.* **71**, 1222–1229.

Mewes, M.-O., *et al.* 1996*a* *Phys. Rev. Lett.* **77**, 416–419.

Mewes, M.-O., *et al.* 1996*b* *Phys. Rev. Lett.* **77**, 988–991.

Monroe, C., Swann, W., Robinson, H. & Wieman, C. 1990 *Phys. Rev. Lett.* **65**, 1571–1574.

Myatt, C. J., Newbury, N. R., Ghrist, R. W., Loutzenhiser, S. & Wieman, C. E. 1996 *Opt. Lett.* **21**, 290–292.

Myatt, C. J., Burt, E. A., Ghrist, R. W., Cornell, E. A. & Wieman, C. E. 1997 *Phys. Rev. Lett.* **78**, 586–589.

Newbury, N. R. & Wieman, C. E. 1996 *Am. J. Phys.* **64**, 18–20.

Sesko, D., Walker, T., Monroe, C., Gallagher, A. & Wieman, C. 1989 *Phys. Rev. Lett.* **63**, 961–964.

Sesko, D., Walker, T. & Wieman, C. 1991 *J. Opt. Soc. Am.* B **8**, 946–958.

Walker, T., Sesko, D. & Wieman, C. 1990 *Phys. Rev. Lett.* **64**, 408–411.

Wieman, C. E. & Chu, S. (eds) 1989 *J. Opt. Soc. Am.* B **6**.

PHILOSOPHICAL TRANSACTIONS OF THE ROYAL SOCIETY A MATHEMATICAL, PHYSICAL & ENGINEERING SCIENCES